JOURNAL OF OPTOELECTRONICS AND ADVANCED MATERIALS Vol. 9, No. 6, June 2007, p. 1829 - 1832

Characterisation of magnetic iron oxide in hydroxyapatite

M. BIRSAN[*], D. PREDOI[a], C. BIRSAN, C. E. SECU[a], E. ANDRONESCU
University POLITEHNICA of Bucharest, Faculty of Applied Chemistry and Materials Science, Department of Science and Engineering of Oxide Materials and Nanomaterials1 – 7, Polizu Street, 011061, PO – BOX 12-134, Bucharest 1, Romania
[a]National Institute for Physics of Materials, P.O. Box MG 07, Bucharest, Măgurele, Romania

In order to be used for medical applications, a material must exhibit many specific characteristics, of which the most fundamental is related to biocompatibility. Lately, the iron oxide nanoparticles are preferred for biomedical applications because they present a superparamagnetic behaviour at room temperature. The preparation method and conditions of iron oxide nanoparticles represents some of the most important challenges that will determine the particle size and shape, the size distribution, the surface chemistry of the particles and consequently their magnetic properties. The samples were characterized by X-ray diffractions (XRD), transmission electron microscopy (TEM) and infrared spectroscopy.

(Received November 14, 2006; accepted April 26, 2007)

Keywords: Nanoparticles, Iron oxide, Hydroxyapatite, Bioceramic

1. Introduction

Bioceramic materials based magnetic particles are used in several biomedical applications [1-4]. Real applications of ferromagnetic material obtained by synthetic routes, controlling the size and the morphology in life sciences are distinct at the present time. Ferromagnetic bioceramics were utilised for hyperthermic treatment of bone cancer [5-10].

The hydroxyapatite (HAp) bioceramics are used in reconstitute orthopaedic and dental surgery [11-14]. For many years, HAp have been extensively studied for bone substitute applications [15-17] and studies have shown that the mechanical strength of the ceramics is a function of density, grain size and morphology characteristics [18-21]. The composition of the inorganic component of bone is similar to poorly crystalline, calcium deficient, carbonated apatite [22].

In this study, magnetite (Fe_3O_4) was synthesized by coprecipitation method. The magnetite powders were introduced in hydroxyapatite (HAp) and sintering at different temperatures. In addition, the structural properties of magnetite and HAp with Fe_3O_4 were studied through X-ray diffraction, IR spectroscopy and transmission electron microscopy (MET).

The structural properties are important due to their possible applications as biological sensors.

2. Experimental

Sample preparation

Magnetic nanoparticles were prepared according to the following procedure: ferrous chloride tetrahydratate ($FeCl_2{\cdot}4H_2O$) in 2M HCl and ferric chloride hexahydratate ($FeCl_3{\cdot}6H2O$) were mixed at room temperature (Fe2+/Fe3+=1/2). The mixture was dropped into 200 ml aqueous ammonia solution (0,6M) in 30 min with vigorous stirring. The pH values of the reaction mixture were kept in the range of 10-11 with the addition of ammonium hydroxide solution 3M. The resulting nanoparticles were separated by centrifugation at 10000 rot/min 30 min. The product was washed with deoxygenated water and dried in air. The resulting nanoparticles were confirmed to be Fe3O4 by X-ray diffraction.

Two series of samples were prepared in the system hydroxyapatite (HAp), Fe_3O_4 (sample H1 and sample H2). Powders of HAp (65 weight %) and Fe_3O_4 nanoparticles (35 weight %) were milled 1h at 180 rot / min in a dried environment. The obtained powders were then thermally treated at 600^0C, with 1 hour (H1) and, respectively, 3 hours (H2) soaking time.

Sample characterization

The samples were characterized by X-ray diffraction (XRD) with a Philips PW1050 X- ray powder diffractometer using CuKα incident radiation. An estimation of crystallite sizes was done from the width of the diffraction using the Scherrer formula.

Transmission electron microscopy (TEM) experiments were performed with a JEOL 2000FX operating at an accelerating voltage of 200 kV. Sample for TEM were performed on copper grids coated with a carbon support film by evaporating a drop of particles dispersions.

Using a Scanning Electron Microscope with, type HITACHI S2600N with EDAX / 2001 device, operating at 25kV in vacuum, the structure and morphology of the samples were studied. The SEM studies were performed on powder samples.

IR spectroscopic studies were performed in the range 1800-400 cm-1 using a FTIR Spectrum BX spectrometer. Samples dehydrated at room temperature were pelleted with dried KBr.

3. Results and discussion

Fig. 1 shows the X-ray diffraction patterns of iron oxide synthesized. The pattern could be indexed to cubic spinel structure with lattice parameter of a_o= 8.392 Å which is close to that of the reported value (a_o= 8.395 Å) of magnetite phase [23]. The d values calculated from the XRD patterns conformed more close to that of standard Fe_3O_4 [ASTM Card No. 19-629].

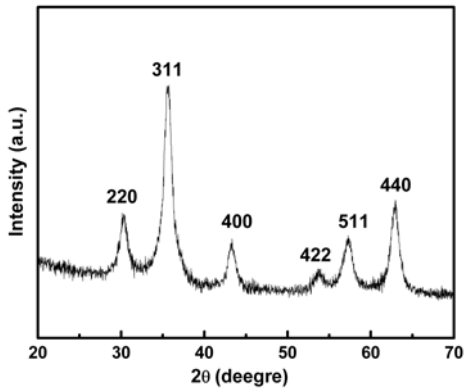

Fig. 1. X-Ray diffraction pattern of Fe_3O_4 nanoparticles.

XRD patterns of the hydroxyapatite (HAp) with different Fe_3O_4 additions are shown in Fig. 2. The XRD spectra, for samples heated in air a 600 ^oC for 1 h (H1) and 3 h (H2) shows the phase peaks corresponding to Fe_3O_4 and a mixture of HAp and β- TCP (β-tricalcium phosphate). This confirms that the stoichiometry of HAp very much determines its thermal stability and non-stoichiometric HAp readily decompose to β- TCP upon heat- treatment to 1000 ^oC, as is known in calcium phosphates literature [24].

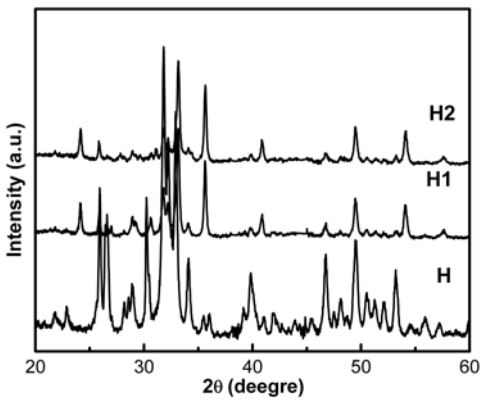

Fig. 2. X-Ray diffraction pattern of HAp (H), sample H1 and sample H2.

Transmission Electron Microscopy observations were used to characterize the state of aggregation and size distributions. Fig. 3 shows a TEM image that was used to determine particle size distribution and morphology for Fe_3O_4 nanoparticles. The nanoparticles are nearly spherical and have an average diameter of 8 nm.

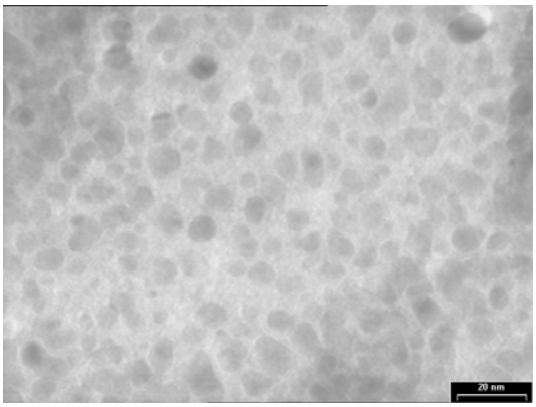

Fig. 3. Transmision electron microscopy (MET) of the magnetite nanoparticles.

Fig. 4 shows the SEM micrograph of samples H1 and H2. The SEM images obtained for the powders H1 and H2 are showing smaller magnetite grains attached to the surface of the hydroxyapatite grains.

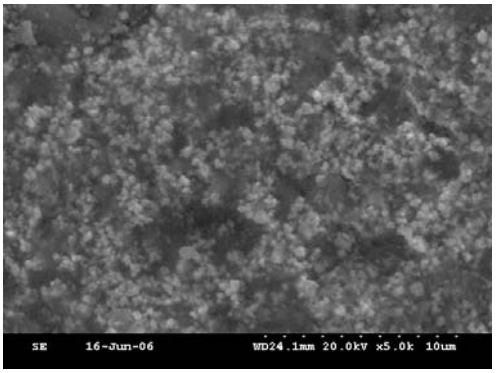

(a) SEM image (x 5.000) for H1

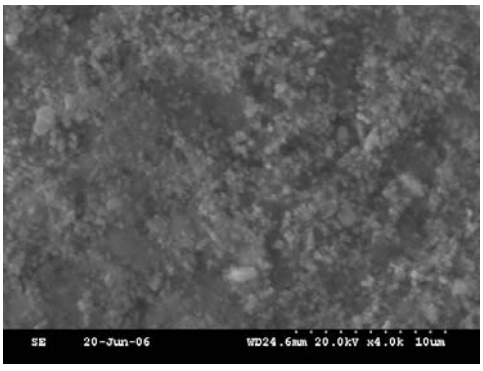

(b) SEM image (x 4.000) for H2

Fig. 4. The SEM micrographs of samples H1 (a) and H2 (b) powder.

Fig. 5 show the FTIR spectra for magnetite and the infrared spectra of the sample H1 and H2 between 4000 and 400 cm^{-1}. Since magnetite has an inverse spinel type structure, it shows bands indicating the vibration M_{Th}-O-M_{Oh} (ν1≈ 550 cm^{-1}) and M_{Th}-M_{Oh} (ν3≈ 350-400 cm-1), where M_{Th} and M_{Oh} correspond to the metal occupying tetrahedral and octahedral positions respectively [25-26]. The stretching vibration ν (Fe-O) correspond of tetrahedral iron atoms. The band at 3500 cm^{-1} and the bands at 1640 cm^{-1} is due to the vibrations of hydrogen-bonded water molecules adsorbed on the surface [27].

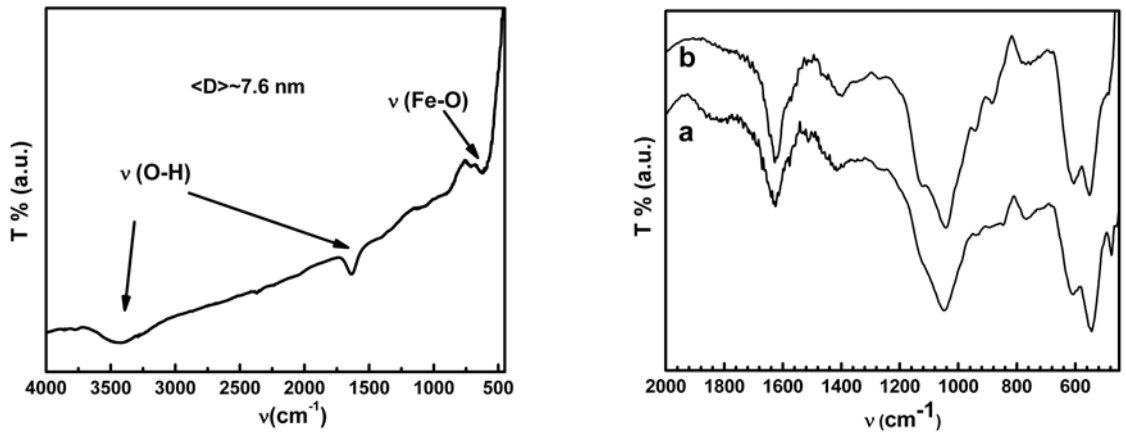

Fig. 5. FTIR spectra of magnetite (<D>≈ 7.6 nm) and FTIR spectra of sample H1 (a) and sample H2 (b).

The infrared spectra of the sample H1 and H2 (Fig. 5) show the vibration modes of Fe_3O_4 and of HAp. In this specra, the characteristic bands of HAp are observed [28-30].The band at 470 cm^{-1} (ν2) can be attributed to Fe_{Oh}-O. The bands at 550-600 cm^{-1} can be attributed to the M_{Th}-O-M_{Oh} (ν1) and to the PO_4^{3-} ions (ν4). The shoulder at 960 cm^{-1} (ν1) and the band at 1040 cm^{-1} (ν3) can be attributed to the PO_4^{3-} ions. Vibrations associated to the vibrations of hydrogen-bonded water molecules adsorbed on the surface are detected by the band 1640.The band at 1419 cm^{-1} arise from vibrations of CO_3^{-2} ions. The presence of carbon modes in commercial sample is an indication that carbon is also an impurity in this sample from the preparation process, which is not detected in the X-ray.

4. Conclusions

In this paper we did a study on the structural properties of magnetite nanoparticles and bioceramic hydroxyiapatite doped with magnetite.

The magnetite nanoparticles were synthesised by the coprecipitation method. Two biomaterials composed of hydroxyapatite and magnetite nanoparticles were prepared and sintered at 600 ^oC with 1h and, respectively 3h soaking time.

The obtained XRD and FTIR patterns confirmed the presence of the desired biocompatible and ferromagnetic components in both samples.

Acknowledgments

This work was supported by grants from National Recherch Program (CEEX_24/2005 VIASAN Program) of Romania. We gratefully acknowledge Institut de Chimie de la Matière Condensée de Bordeaux for the use of theirs laboratories in the sample characterisation.

References

[1] M. Ikenaga, K. Ohura, T. Nakamura, Y. Kotoura, T. Yamamuro, M. Oka, Y. Ebisava, T. Kokubo, Bioceramics **4**, 255 (1991).
[2] K. Ohura, M. Ikenaga, T. Nakamura, T. Yamamuro, Y. Ebisava, T. Kokubo, Y. Kotoura, M. Oka, J. Appl. Biomat **2**, 159 (1991).
[3] T. Kokubo, Y. Ebisava, Y. Sugimoto, M. Kiyama, K. Ohura, T. Yamamuro, M. Hiraoka, M. Abe, Bioceramics **5**, 213 (1992).
[4] Th. Leventouri, A. C. Kis, J. R. Thompson, I. M. Anderson, Biomaterials **26**, 4924 (2005).
[5] K. Ohura, M. Ikenaga, T. Nakamura, T. Yamamuro, Y. Ebisava,T. Kokubo, Y. Kotoura, M. Oka, Bioceramics **3**, 225 (1992).
[6] Y. Ebisava, T. Kokubo, K. Ohura, T. Yamamuro, J. Mater. Sci: Mater Med **4**, 225 (1993).
[7] M. Ikenaga, K. Ohura, T. Yamamuro, Y. Kotoura, M. Oka, T. Kokubo, J. Orthop. Res. **11**, 849 (1993).
[8] Y. Ebisava, F. MiYaji, T. Kokubo, K. Ohura, T. Nakamura, J. Biomater **18**, 1277 (1997).
[9] K. Takegami, T. Sano, H. Wakabayashi, J. Sodona, T. Yamazaki, S. Morita, T. Shibuya, A. Uchida,

J. Biomed. Mater. Res. **43**, 210 (1998).
[10] U. Gross, V. Strunz, J. Biomed. Mater. Res. **19**, 251 (1985).
[11] R. Z. LeGeros, J. P. LeGeros, in L. L. Hench, J. Wilson (Eds.), „An introduction to Ceramics, World Scientific, Singapore, 1993.
[12] K. de Groot, Ceram. Int. **19**(5), 363 (1993).
[13] S. Qu, W. Chen, J. Weng, X. Zhang, in: Y. Urpo, H. Anderson (Eds.), Bioceramics, 7, Butterworth-Heinemann, London, 1994.
[14] C. Lavernia, J. schoenung, Ceram. Bull. **70**(1), 95 (1991).
[15] M. Bohner, Injury **31**(4), 37 (2003).
[16] W. Suchanek, M. Yoshimura, J. Mater. Res. **13**(1), 94, (1998).
[17] J. W. Reid, L.Tuck, M. Sayer, K. Fargo, J. A. Hendry, Biomaterials **27**, 2916 (2006).
[18] N. Thangamani, K. Chinnakali, F. D. Gnanam, Ceram. Int. **28**(4), 355 (2002).
[19] N. J. Petch, J. Iron Steel Inset. **174**(1), 25 (1953).
[20] F. P. Knudsen, J. Am. Ceram. Soc. **42**(8), 376 (1959).
[21] R. W. Rice, J. Mater. Sci. **28**(8), 2187 (1993).
[22] V. Sergo, O. Sbaizero, D. R. Clarke, Biomaterials **18**, 477 (1997).
[23] G. Visalakski, G. Venkateswaran, S. K. Kulshreshtha, P. H. Moorthy, Mater. Res. Bull. **28**, 829 (1993).
[24] N. Kivrak, A. Tas Cuneyt, J. Am Ceram Soc. **81**(9), 2245 (1998).
[25] E. Barrodo, F. Prieto, J. Medina, F. A. Lopez, J. Alloys. Compd. **335**, 203 (2002).
[26] J. L. Martin de Vidales, A. Lopez-Delgado, E. Vila, F. A. Lopez, J. Alloys. Compd. **287**, 276 (1999).
[27] M. L. Hair, J. Non-Cryst. Solids **19**, 299 (1975).
[28] I. F. Vasconcelos, J. Mater. Sci. **36**, 587 (2001).
[39] M. N. Taravel, Biomaterials, **16**(11), 865 (1995).
[30] C. C. Silva, H. G. B. Rocha, F. N. A. Freire, M. R. P. Santos, K. D. A. Saboia, J. C. Goes, A. S. B. Sombra, Materials Chemistry and Physics **92**, 260 (2005).

*Corresponding author: birsan_1@yahoo.com